

Sextupole Corrections for the SNS Ring

C. J. Gardner

January 1998

Collider Accelerator Department
Brookhaven National Laboratory

U.S. Department of Energy

USDOE Office of Science (SC)

Notice: This technical note has been authored by employees of Brookhaven Science Associates, LLC under Contract No. DE-AC02-98CH10886 with the U.S. Department of Energy. The publisher by accepting the technical note for publication acknowledges that the United States Government retains a non-exclusive, paid-up, irrevocable, world-wide license to publish or reproduce the published form of this technical note, or allow others to do so, for United States Government purposes.

DISCLAIMER

This report was prepared as an account of work sponsored by an agency of the United States Government. Neither the United States Government nor any agency thereof, nor any of their employees, nor any of their contractors, subcontractors, or their employees, makes any warranty, express or implied, or assumes any legal liability or responsibility for the accuracy, completeness, or any third party's use or the results of such use of any information, apparatus, product, or process disclosed, or represents that its use would not infringe privately owned rights. Reference herein to any specific commercial product, process, or service by trade name, trademark, manufacturer, or otherwise, does not necessarily constitute or imply its endorsement, recommendation, or favoring by the United States Government or any agency thereof or its contractors or subcontractors. The views and opinions of authors expressed herein do not necessarily state or reflect those of the United States Government or any agency thereof.

SEXTUPOLE CORRECTIONS FOR THE SNS RING

BNL/SNS TECHNICAL NOTE

NO. 041

C. J. Gardner

January 14, 1998

ALTERNATING GRADIENT SYNCHROTRON DEPARTMENT
BROOKHAVEN NATIONAL LABORATORY
UPTON, NEW YORK 11973

Sextupole Corrections for the SNS Ring

C.J. Gardner

January 14, 1998

1 Introduction

The Accumulator Ring [1] for the proposed Spallation Neutron Source (SNS) is designed to operate with horizontal and vertical tunes (Q_x and Q_y) between 5 and 6. Several second, third and fourth-order resonance lines cross this region, and, because the ring will operate at very high intensities for which stringent limits on losses will be imposed, the possibility of beam loss due to the presence of these resonances must be considered. Although the space-charge tune spread of the beam is expected to be small (at most 0.1), a number of resonance lines are sufficiently close to the nominal working point ($Q_x = 5.82$, $Q_y = 5.80$) to be of concern. Other lines in the region may also be of concern if one wants to have room to maneuver the tunes. In this report we focus on the $3Q_x = 17$ and $Q_x + 2Q_y = 17$ resonances which are excited by sextupole fields in the ring.

2 The Ring Lattice and Correction Elements

The ring lattice [2, 3, 4] consists of four superperiods, each containing a 90° arc and a long straight section. The four superperiods are labeled A, B, C, D and run sequentially along the beam direction from the beginning of one arc to the next. The order of magnets in each superperiod X is DHX1, QVX1, DHX2, QHX2, ..., DHX8, QHX8, QVA9, QHX10, QVX11, QHX12, where D and Q denote dipoles and quadrupoles, and H and V refer to the horizontal and vertical planes. The long straight section in superperiod X runs from QHX8 through QHX12.

To compensate for the small unavoidable field imperfections and magnet alignment errors that can lead to resonance excitation, the ring will have a

set of correction elements consisting of horizontal and vertical dipoles, skew quadrupoles, sextupoles, skew sextupoles and octupoles. Trim windings on the lattice quadrupoles will allow for any necessary quadrupole corrections. Correction dipoles and skew quadrupoles will be mounted downstream of the position monitor at each quadrupole with the dipole and skew quadrupole windings wound on the same core. Sextupole correctors will be located downstream of quadrupoles QHX8 and QVX9 in each superperiod and will be labeled SHX8 and SVX9 respectively. In the calculations carried out for this report, the sextupole correctors were taken to be thin elements located at the downstream ends of the quadrupoles; the integrated strength of each sextupole was taken to be 1.0×10^{-2} T/m per Amp.

3 Sextupole Strings

For the correction of random sextupole errors that can excite the $3Q_x = 17$ and $Q_x + 2Q_y = 17$ resonances, it is necessary to connect the sextupoles together in series strings that produce azimuthal harmonic 17. Thus we define the following four strings:

$$\text{SHY} = \text{SHA8} - \text{SHC8}, \quad \text{SHZ} = \text{SHB8} - \text{SHD8}$$

$$\text{SVY} = \text{SHA9} - \text{SHC9}, \quad \text{SVZ} = \text{SHB9} - \text{SHD9}$$

Here the $-$ signs indicate the relative polarities of the sextupoles. The two sextupoles in each string are spaced two superperiods apart and are separated by an azimuthal angle of π . They are excited with opposite polarities, and therefore produce only harmonics 1, 3, 5, 7, 9, 11, and so on, as discussed in Ref. [5]. At the 17th harmonic, the strings provide orthogonal correction of the real and imaginary parts of the $3Q_x = 17$ and $Q_x + 2Q_y = 17$ resonance excitation coefficients. Since only odd harmonics are produced, the strings will not affect the machine chromaticities. Note that the sextupoles in the SHY and SHZ strings are placed near Horizontal beta maximums while those in the SVY and SVZ strings are near Vertical beta maximums. This allows for simultaneous and independent correction of the two resonance lines.

4 Correction of the $3Q_x = 17$ and $Q_x + 2Q_y = 17$ Resonances

To test the ability of the sextupole strings to compensate random sextupole errors that can excite the $3Q_x = 17$ and $Q_x + 2Q_y = 17$ resonances, we use the Efield command of the MAD code [6, 7, 8] to generate Gaussian distributions of sextupole errors in the ring dipoles. We take the RMS deviation of each distribution to be a sextupole integrated strength of 0.1 T/m and impose a cutoff of 2.5 standard deviations. The effect of sextupole errors on particle motion can be determined by examining phase space contours obtained with the tunes near the resonances. Figure (1) shows the horizontal phase space contours produced with NO sextupole fields in the ring. Here the tunes have been adjusted to be $Q_x = Q_y = 5.667667$ and five particles with initial horizontal coordinates $x = 5, 10, 15, 20, 25$ mm and momenta $p_x = 0$ have been launched from a point just upstream of quadrupole QHA10 and tracked with the MAD Code for 400 turns around the ring. The contours in this case are just the Courant-Snyder ellipses one expects for a ring with no nonlinear fields. (The horizontal Courant-Snyder parameters at the launching point are $\alpha_x = -2.012$, $\beta_x = 18.539$ m.) The area enclosed by the largest-amplitude contour is 170π mm mr; somewhat larger than the nominal beam emittance of 120π mm mr, but smaller than the 330π mm mr acceptance. Figure (2) shows the contours obtained with the same initial conditions but with a sextupole error distribution generated from a seed of 7777. Because the tunes are close to the $3Q_x = 17$ and $Q_x + 2Q_y = 17$ resonances, we see significant distortion of the contours as the amplitude of the phase space motion increases. Note that the initial vertical coordinates and momenta were taken to be zero here, so there is no vertical motion in this case; the particle remains in the magnetic midplane.

To see the effect of the sextupole errors on motion in the vertical plane, we again set the tunes to be $Q_x = Q_y = 5.667667$ but now launch the five particles with initial vertical coordinates $y = 5, 10, 15, 20, 25$ mm and momenta $p_y = 0$, and with zero horizontal coordinates and momenta. Figure (3) shows the vertical phase space contours produced with NO sextupole fields in the ring. (The vertical Courant-Snyder parameters at the launching point are $\alpha_y = 0.573$, $\beta_y = 4.853$ m, and the area enclosed by the largest-amplitude contour is 171π mm mr.) Figure (4) shows the contours obtained with the same initial conditions but with a sextupole

error distribution generated from a seed of 7777. Here again we see significant distortion of the contours as the amplitude of the phase space motion increases. In this case the $Q_x + 2Q_y = 17$ resonance couples the motion in the two planes, so we must also look in the horizontal plane; Figure (5) shows the motion there.

To compensate for the sextupole errors, we first adjust the currents in the sextupole strings SHY and SHZ to minimize the distortion of the Horizontal phase space contours shown in Figure (2). Then we adjust the currents in SVY and SVZ strings to minimize the distortion of the Vertical phase space contours shown in Figure (4). Iterating a couple of times we find that we can correct the distortion in both planes with currents of +6, -5, -3, and +15 Amps in the SHY, SHZ, SVY, and SVZ strings respectively. Figures (7) and (8) show the phase space contours obtained with these corrections; they are indistinguishable from those obtained with no sextupole fields. Figure (6) shows the motion in the horizontal plane for the case in which particles were launched in the vertical plane (with the corrections listed above). Comparing with Figure (5) we see that the coupling effect of the $Q_x + 2Q_y = 17$ resonance has been corrected.

The results of carrying out the above analysis for several different seeds are summarized in Table I.

Table I: Resonance Correction $Q_x = Q_y = 5.667667$ (Currents in Amps)				
Seed	ISHY	ISHZ	ISVY	ISVZ
7777	+6	-5	-3	+15
6666	+4	-5	-14	-3
5555	-1	+1	0	+3
4444	+4	-4	-12	-6
3333	-8	-2	-1	0
2222	-7	+2	+6	+6
1111	+7	-6	-13	+5
0111	+7	-10	-12	+3

5 Comments

The primary purpose of the preceding analysis was to show that, for the particular placement of sextupole correctors we have chosen, we are able to correct the phase space distortions due to the $3Q_x = 17$ and $Q_x + 2Q_y = 17$

resonances. In order to demonstrate this, we have assumed sextupole errors much larger than those expected on the basis of the field purity achievable in the ring dipoles. The results show that, even with errors this large, sextupoles similar to those employed in the AGS Booster are more than adequate for the SNS Ring. (The Booster sextupoles have an integrated strength of 1.3×10^{-2} T/m per Amp and are powered with bipolar 50 Amp power supplies. An integrated strength of 1.0×10^{-2} T/m per Amp was assumed for the correctors used in the analysis reported here.)

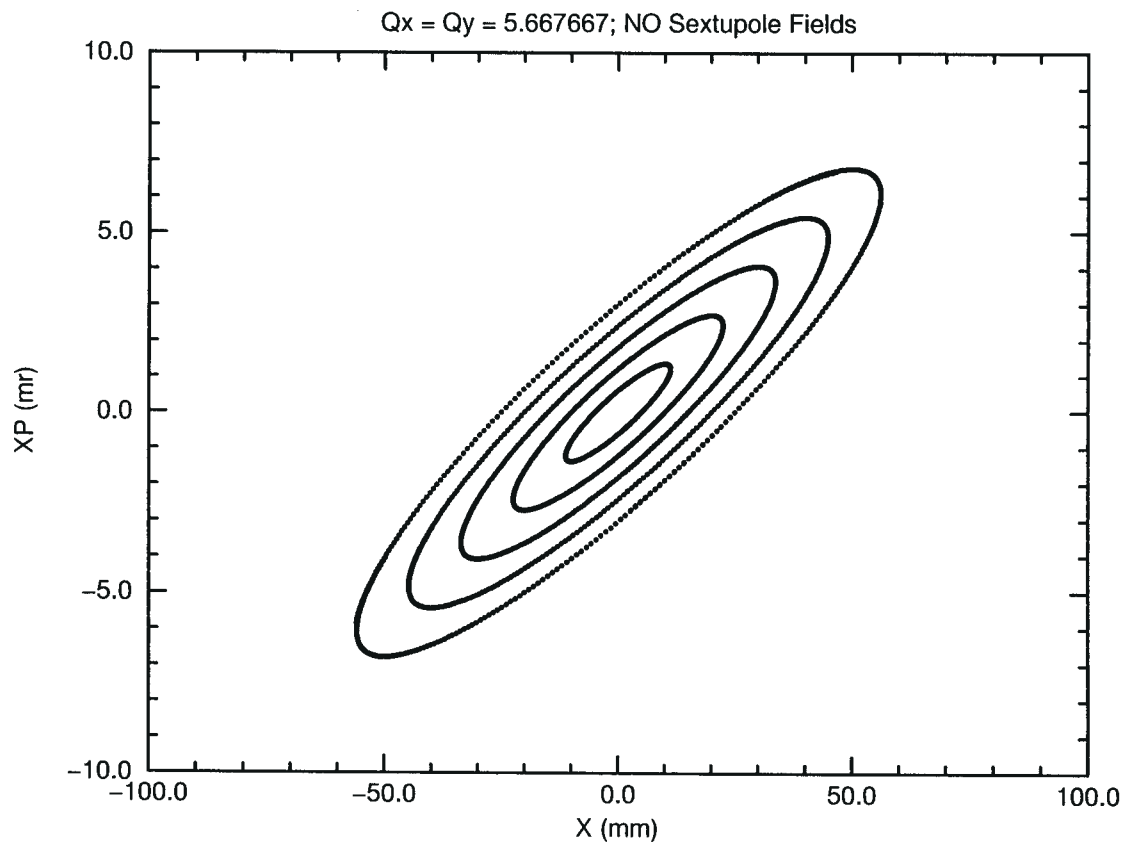
6 Acknowledgement

As always, I would like to thank Jim Niederer for his help and advice in using the MAD code.

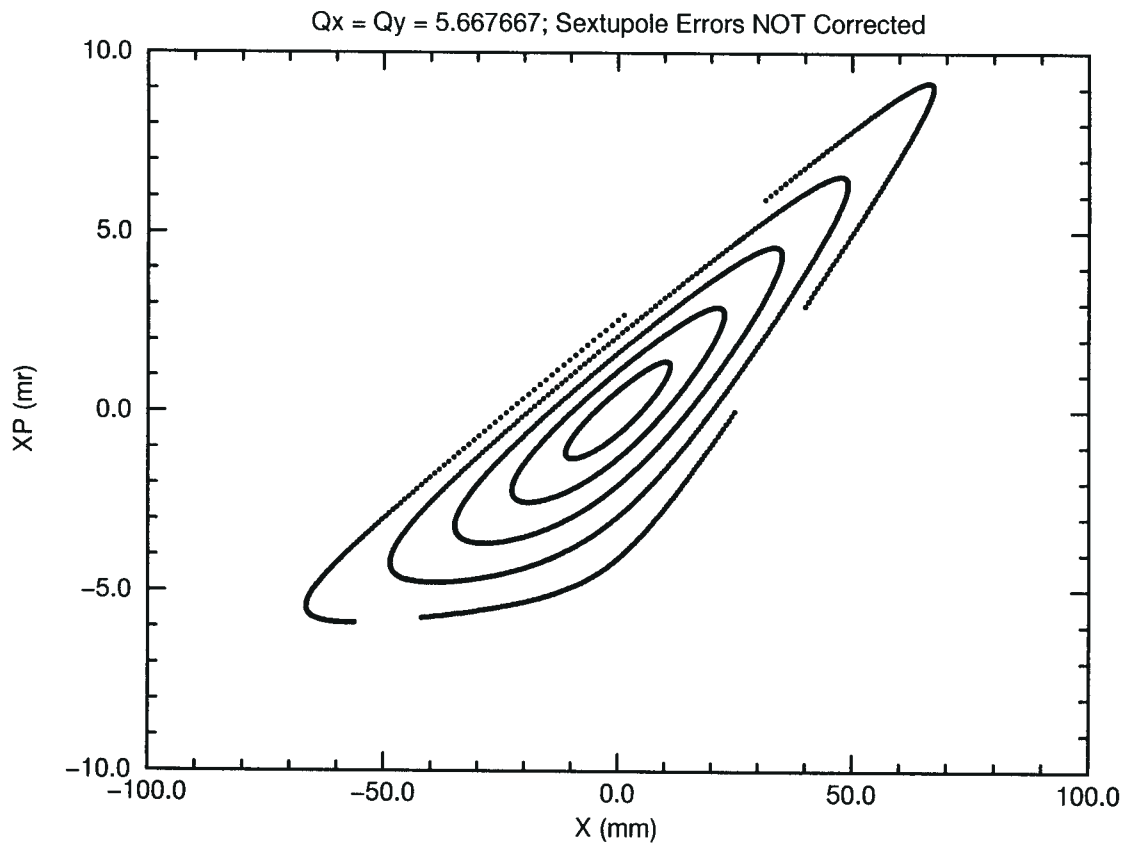
7 References

1. W.T. Weng, et. al., "Accumulator Ring Design for the NSNS Project", Proceedings of the 1997 Particle Accelerator Conf., Vancouver, B.C., Canada, May 12–16, 1997.
2. Y.Y. Lee, "The 4 Fold Symmetric Lattice for the NSNS Accumulator Ring", BNL/NSNS Tech. Note No. 026, February 19, 1997.
3. C.J. Gardner, Y.Y. Lee, and A.U. Luccio, "Accumulator Ring Lattice for the National Spallation Neutron Source", Proceedings of the 1997 Particle Accelerator Conf., Vancouver, B.C., Canada, May 12–16, 1997.
4. C.J. Gardner, "Some Notes on Tuning the NSNS Ring Lattice", BNL/NSNS Tech. Note No. 037, August 12, 1997.
5. C.J. Gardner, "Some Notes on the Placement of Correctors" BNL/SNS Tech. Note No. 040, December 29, 1997.
6. H. Grote and F.C. Iselin, "The MAD Program Version 8.4 User's Reference Manual", CERN/SL/90–13 (AP), 27 August 1991.
7. J. Niederer, "BNL MAD Program Notes—Fmatch: Enhanced Matching Commands", AGS/AD/Tech. Note No. 436, June 3, 1996.
8. J. Niederer, "BNL MAD Program Notes—Upgrade to Version 7C", AGS/AD/Tech. Note No. 463, July 14, 1997.

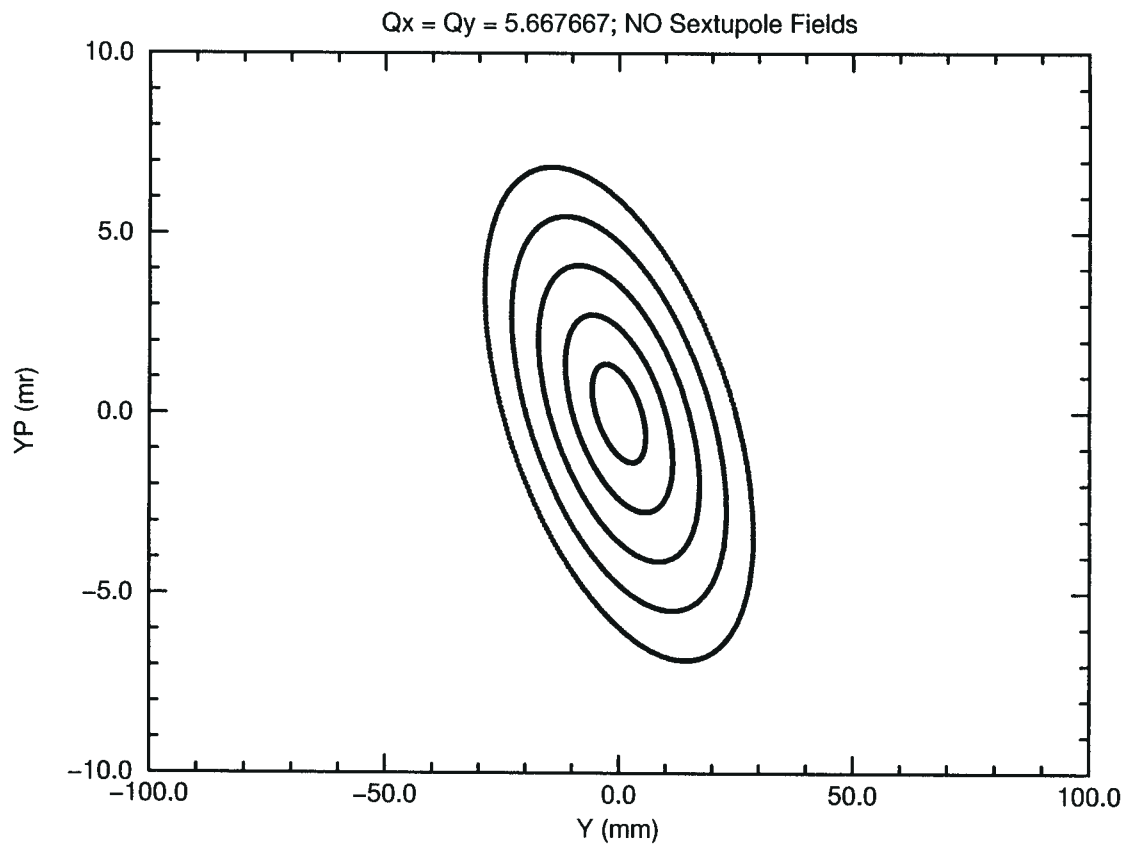
Horizontal Phase Space Contours: Figure 1



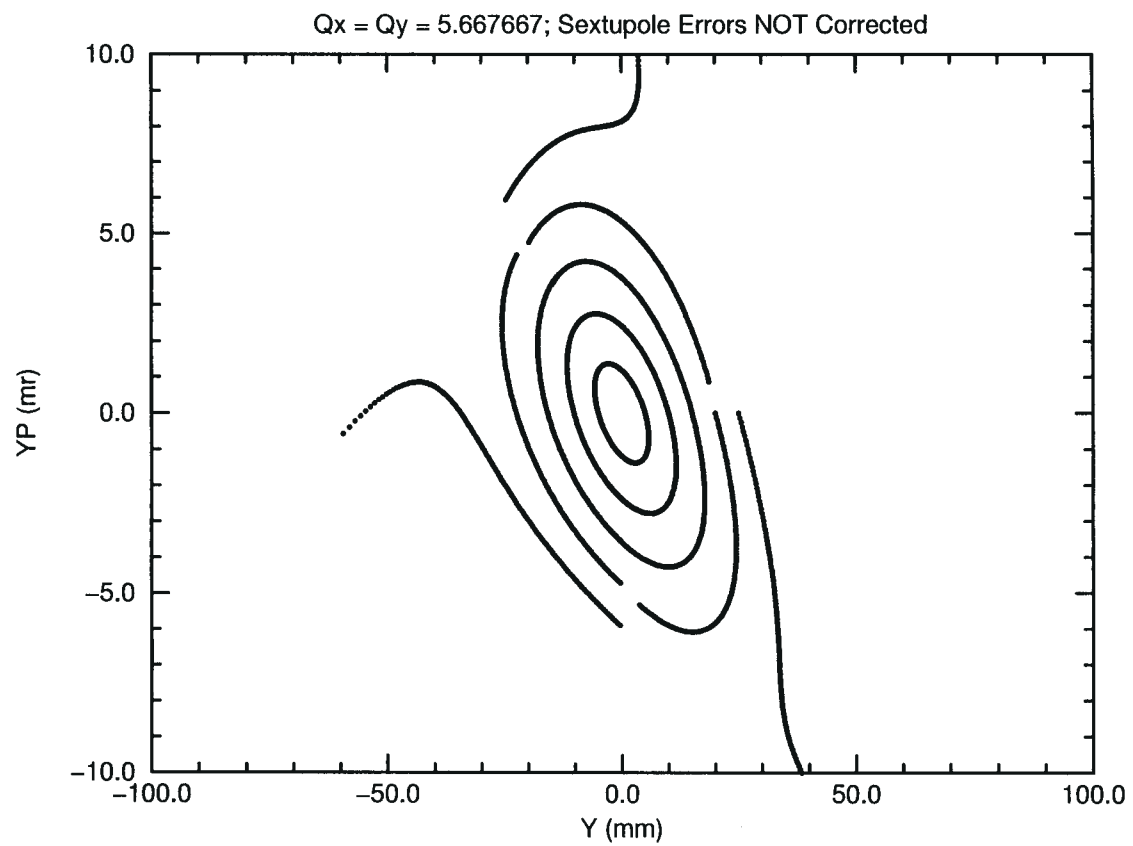
Horizontal Phase Space Contours: Figure 2



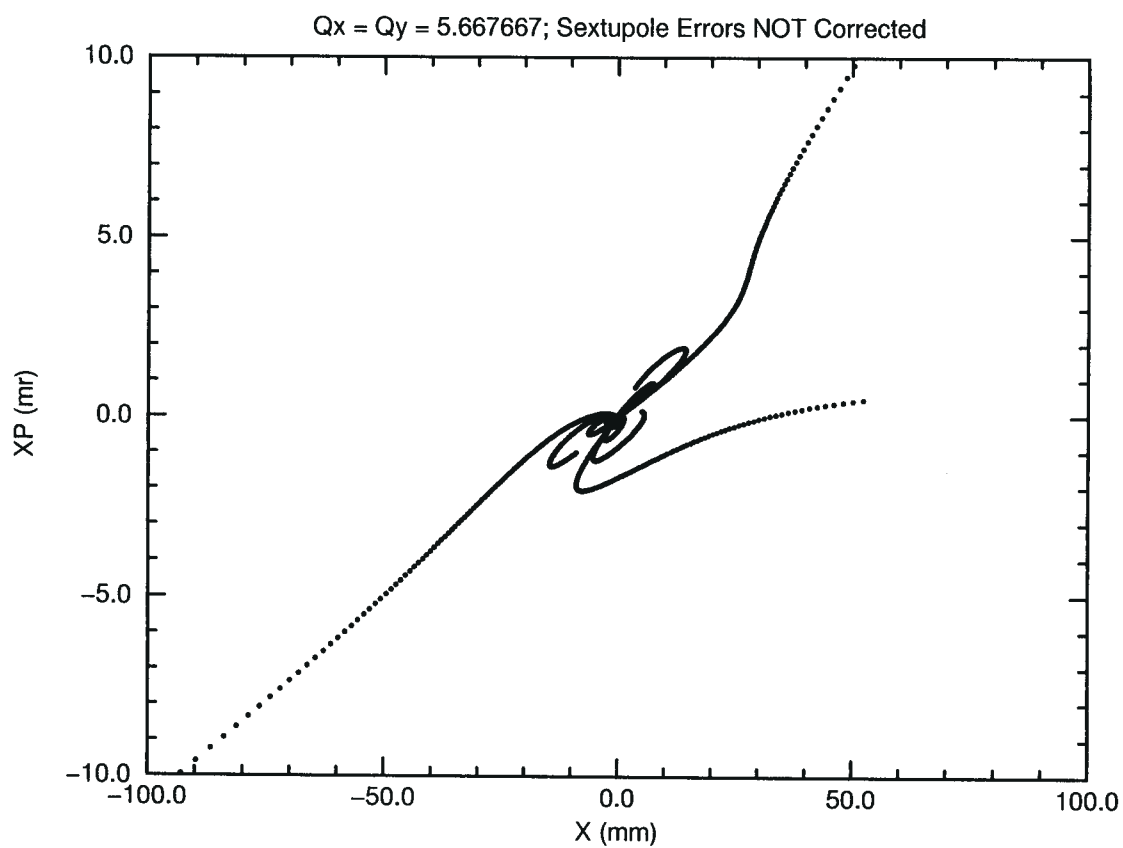
Vertical Phase Space Contours: Figure 3



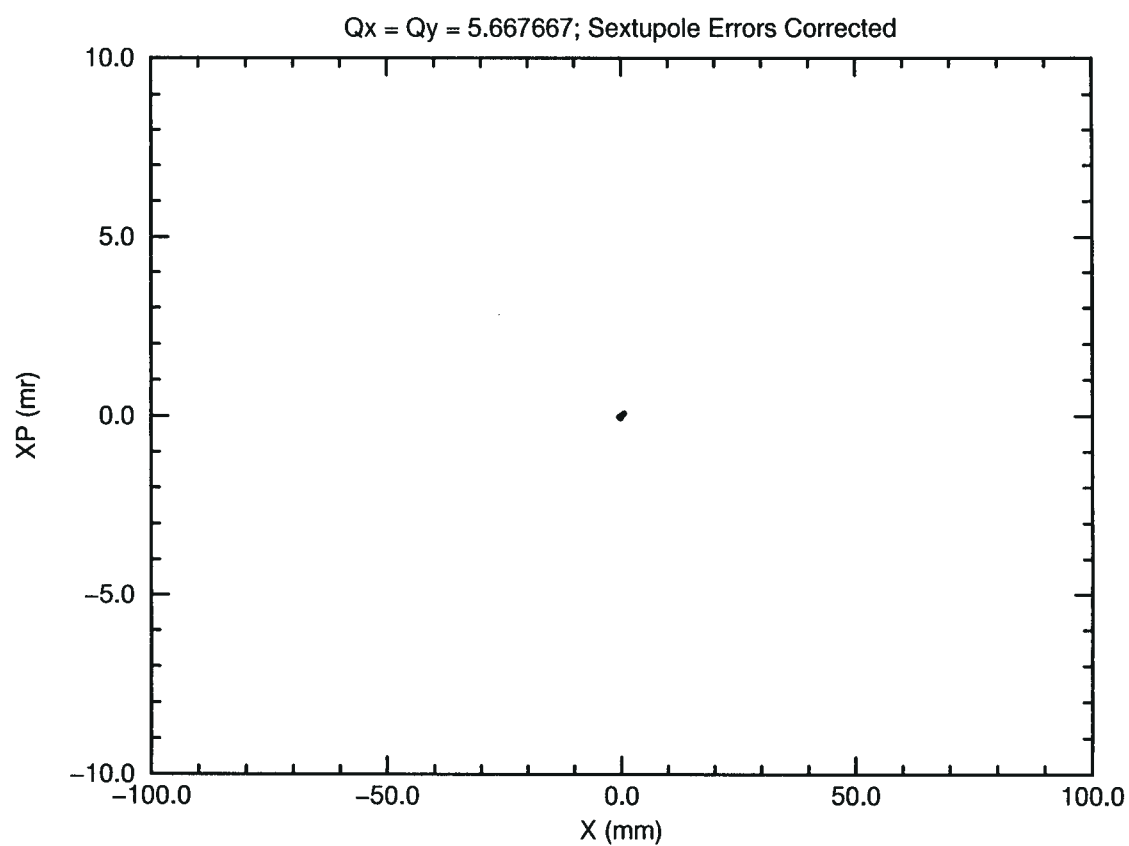
Vertical Phase Space Contours: Figure 4



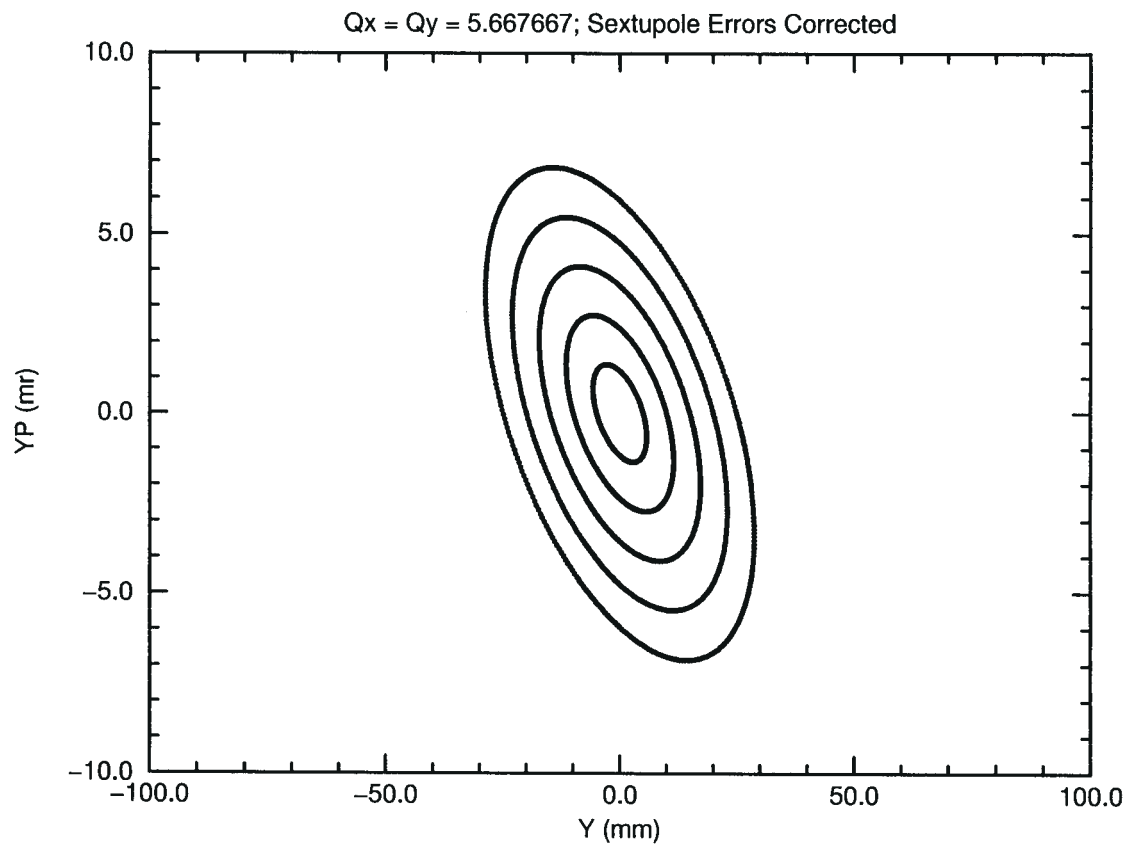
Motion in Horizontal Phase Space: Figure 5



Motion in Horizontal Phase Space: Figure 6



Vertical Phase Space Contours: Figure 7



Horizontal Phase Space Contours: Figure 8

